J. Fluid Mech. (1988), *vol.* 186, *pp.* 393–417
Printed in Great Britain

Propulsion of a foil moving in water waves

By JOHN GRUE, ASBJØRN MO AND ENOK PALM
Department of Mechanics, University of Oslo, Norway

(Received 26 August 1986 and in revised form 8 July 1987)

Propulsion of a foil moving in the water close to a free surface is examined. The foil moves with a forward speed U and is subjected to heaving and pitching motions in calm water, head waves or following waves. The model is two-dimensional and all equations are linearized. The fluid is assumed to be inviscid and the motion irrotational, except for the vortex wake. The fluid layer is infinitely deep.

The problem is solved by applying a vortex distribution along the centreline of the foil and the wake. The local vortex strength is found by solving a singular integral equation of the first kind, which appropriately is transformed to a non-singular Fredholm equation of the second kind. The vortex wake, the forward thrust upon the foil and the power supplied to maintain the motion of the foil are investigated. The scattered free surface waves are computed. For moderate values of $U\sigma/g$ (U is forward speed of the foil, σ is frequency of oscillation, g is acceleration due to gravity) it is found that the free surface strongly influences the vortex wake and the forces upon the foil. When the foil is moving in incoming waves it is found that a relatively large amount of the wave energy may be extracted for propulsion. As an application of the theory the propulsion of ships by a foil propeller is examined. The theory is compared with experiments.

1. Introduction

Recently, various experiments have been performed in order to examine the possibilities of utilizing the energy in ocean waves for propulsion of ships (Jakobsen 1981), Isshiki, Murakami & Terao (1984). One or two hydrofoils have been fixed to the ship. When the ship is heaving and pitching in incoming waves, head waves or following waves, the hydrofoils will also perform a heaving motion. Since the ship (and the foil) is moving forward, the heaving of the foil will produce a forward thrust on the foil, and the foil will act as a propeller. This is easily seen to be true for a deeply submerged foil performing a low-frequency heave motion. In this case the total force on the foil from the fluid is approximately equal to the lift, and the horizontal component of the force gives a forward thrust in both upward and downward motion.

In a pure heaving motion, however, the angle between the foil and the path of the foil, the angle of attack, may easily be so large that stall occurs. To avoid stall it may therefore be necessary that the foil also performs a pitch motion. This is obtained in the experiments referred to above, by an arrangement of springs. The introduction of a pitch motion has another effect. Assuming that stall does not occur, we shall see that a combined heave and pitch motion usually leads to a larger efficiency, but smaller thrust, than for pure heave motion.

In the present paper we shall be concerned with evaluating mathematically the propulsion of a moving, oscillating foil, sited close to a free surface. It will be assumed

that the aspect ratio is large, so that the problem may be considered as two-dimensional. The foil is assumed to be thin, to have a small camber and to be near horizontal, so that the oscillating part of the fluid motion may be approximated by flow around a thin, horizontal flat plate.

All the equations will be linearized. The corresponding problem with a moving foil oscillating in an unbounded fluid, was studied thoroughly in 1934 (von Kármán & Burgers, 1934). Specially relevant to our problem is a series of papers by Wu (1961, 1971*a*, *b*) on the hydromechanics of swimming propulsion where the optimum oscillating motion of a two-dimensional flat plate is studied. In a later paper Wu (1972) considers the effect of surface waves on a moving, flat plate performing heaving and pitching motions. His theory is approximate since the effects of the free surface upon the foil are neglected. According to his own estimates, his theory is a good approximation if the plate is situated more than twice the chord beneath the free surface. Important also is a work by Lighthill (1970) on aquatic animal propulsion, where he introduces the useful concept of the feathering parameter.

The presence of a free surface complicates the problem considerably. In an unbounded fluid the horizontal thrust equals the mean momentum transport in the vortex wake formed behind the foil. Correspondingly, the wasted energy is solely due to the wake. When a free surface is present, and the foil is sited relatively close to the surface, the generated surface waves may transport a considerable amount of momentum. This momentum transport may be positive or negative, leading to an increase or decrease in the thrust, depending on the properties of the generated waves. The waves always give rise to a considerable amount of wasted energy. Surprisingly, it is found that the total energy waste, composed of waste by the wake and the waves, is nearly independent of the submergence of the foil for moderate and large forward speed. This is not true for the value of the thrust. It will also appear that the effect of the free surface is most pronounced for $U\sigma/g < \frac{1}{4}$ (U is the speed of the foil, σ is the frequency of oscillation, and g is the acceleration due to gravity).

Incoming waves are also accounted for. We shall assume that the period of these waves and the period of the oscillations of the foil are the same. The incoming waves then introduce two new parameters to the problem, viz. the amplitude and phase of the waves. The foil may in this case extract a considerable amount of energy from the waves. We find for example that the thrust may be doubled while the power supplied to the foil reduces to zero when the vertical velocities of the foil and the wave field at the foil are of the same magnitude. The largest extraction of energy is found for incoming following waves and small values of $U\sigma/g$. It is found that up to 75% of the incoming wave energy may be utilized for propulsion.

Sections 2 and 3 concern the mathematical formulation of the problem. The fluid flow is expressed by a distribution of vortices along the foil and the vortex wake. The vortex strength is determined by an ordinary Fredholm equation of the second kind, which is solved by a collocation method as discussed in §4. In §§5 and 6 the impact of the free surface is discussed, for no incoming waves and incoming waves, respectively. In the latter section, the theory is applied to the study of the propulsion of a ship by a foil propeller. The example chosen is a ship of length 40 m moving in long head waves of amplitude 0.5 m. The foil area is 8% of the waterplane area of the ship leading to a forward speed of 8 knots. Finally, in §8 we compare the thrust found by the present theory with the experiments by Isshiki *et al.* (1984). Also the approximate theory of Isshiki (1982) and the present theory are compared.

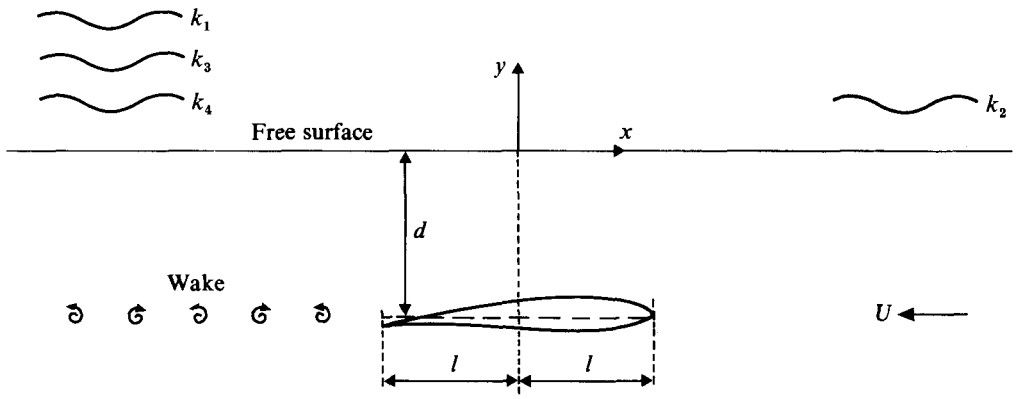

FIGURE 1. Definition sketch.

2. The boundary- values problem

We shall assume that the hydrofoil has a small camber and angle of attack. The foil is also assumed to be thin, though sufficiently rounded at the leading edge to keep the flow from being separated there. For the oscillatory part of the flow the effects of camber and thickness are then only secondary, and the foil may mathematically be replaced by a flat plate. Furthermore the amplitudes of the oscillations of the foil and the amplitudes of the incoming waves are small. Hence, the boundary conditions at the free surface and at the foil may be linearized, even if the foil is placed relatively close to the free surface.

Let coordinates be taken with the origin in the mean free surface of the fluid. The x-axis is horizontal and the y-axis positive upwards, see figure 1. The fluid is assumed incompressible and the motion irrotational. Considering the problem from the frame of reference fixed to the mean position of the foil, the water flows with a horizontal speed U along the negative x-axis. The fluid velocity may then be written

$$\boldsymbol{v} = \nabla\phi - U\boldsymbol{e}_x, \tag{2.1}$$

where ϕ is a velocity potential and $\boldsymbol{e}_x$ is the unit vector along the x-axis. ϕ satisfies the two-dimensional Laplacian

$$\nabla^2\phi = 0. \tag{2.2}$$

We shall consider a fluid of infinite depth. The boundary condition at $y = -\infty$ is then

$$\nabla\phi \to 0, \quad y \to -\infty. \tag{2.3}$$

The boundary condition at the free surface may be written

$$\left(\frac{\partial}{\partial t} - U\frac{\partial}{\partial x}\right)^2\phi + g\frac{\partial\phi}{\partial y} = 0, \tag{2.4}$$

where t denotes time.

Let $\zeta(x,t)$ denote the vertical displacement of the plate. The kinematic boundary condition at the body is then

$$\frac{\partial\phi}{\partial y} = \left(\frac{\partial}{\partial t} - U\frac{\partial}{\partial x}\right)\zeta \quad (y = -d, |x| < l), \tag{2.5}$$

where $2l$ and d are the chord length and depth, respectively.

In the case of an incoming wave the potential is properly divided into two parts

$$\phi = \phi_0 + \phi_1, \tag{2.6}$$

where ϕ_0 is the (known) potential of the incoming wave. The boundary condition (2.5) then takes the form

$$\frac{\partial \phi_1}{\partial y} = \left(\frac{\partial}{\partial t} - U\frac{\partial}{\partial x}\right)\zeta - \frac{\partial \phi_0}{\partial y} \quad (y = -d, |x| < l). \tag{2.7}$$

We shall assume sinusoidal time dependence with period $2\pi/\sigma$. Introducing complex variables, we write

$$\phi = \mathrm{Re}\,[f_c(z)\cos\sigma t + f_s(z)\sin\sigma t], \tag{2.8}$$

where

$$z = x + \mathrm{i}y, \tag{2.9}$$

i is the imaginary unit. $f_c(z)$ and $f_s(z)$ are analytic functions of z. Equation (2.8) may be written in shorter notation by introducing a new imaginary unit j, independent of i and connected to the time variable so that

$$\phi = \mathrm{Re_j}\,\mathrm{Re_i} f(z)\exp(\mathrm{j}\sigma t). \tag{2.10}$$

Here $\mathrm{Re_i}$ and $\mathrm{Re_j}$ denote the real part with respect to i and j, respectively. $f(z)$ is given by

$$f(z) = f_c(z) - \mathrm{j} f_s(z). \tag{2.11}$$

Corresponding to (2.10) we write

$$\left.\begin{aligned} \phi_0 &= \mathrm{Re_j}\,\mathrm{Re_i} f_0(z)\exp(\mathrm{j}\sigma t), \\ \phi_1 &= \mathrm{Re_j}\,\mathrm{Re_i} f_1(z)\exp(\mathrm{j}\sigma t), \end{aligned}\right\} \tag{2.12}$$

with

$$f(z) = f_0(z) + f_1(z), \tag{2.13}$$

$f_0(z)$ is the known complex potential for the incoming wave and $f_1(z)$ is the unknown complex potential due to the presence of the foil.

Finally, at the trailing edge the Kutta condition is applied, ensuring that the velocity is finite at this point. Also, at $x = \pm\infty$ the radiation conditions must be satisfied.

3. The integral equation

To derive an integral equation for the motion we express $f_1(z)$ as a continuous distribution of vortices. The velocity circulation around the foil will oscillate in time due to the periodic motion of the foil or the harmonic incoming waves. Hence, vortices will be shed at the trailing edge, and a vortex wake will be formed behind the foil, extending from the trailing edge to $x = -\infty$ as time goes towards infinity. In the first approximation the wake may be considered to be located along the line $y = -d$. $f_1(z)$ is therefore expressed as an integral from $x = -\infty$ to $x = l$. Let $G(z, z_0)$ denote the complex potential for a vortex of strength unity located at $z = z_0$. $G(z,z_0)$ fulfills the boundary condition at the free surface, the radiation conditions at $x = \pm\infty$ and (2.3) at $y = -\infty$. $G(z, z_0)$ is therefore a Green function. $f_1(z)$ may then be written

$$f_1(z) = \int_{-\infty}^{l} \gamma(\xi)\, G(z, \xi - \mathrm{i}d)\,\mathrm{d}\xi. \tag{3.1}$$

Here γ, which is unknown, is real with respect to i. This is to secure that the boundary condition at $y = 0$ and the radiation conditions are satisfied. γ is, however, complex

in j being of the form $\gamma = \gamma_1 + j\gamma_2$ where γ_1 and γ_2 are real. $G(z, z_0)$ may be derived by an analogous procedure as used by Haskind (1954) in deriving the Green function for a source. It is found that

$$G(z, z_0) = \frac{1}{2\pi i}[\ln(z - z_0) - g(z, z_0)], \tag{3.2}$$

where $g(z, z_0)$ is non-singular in the fluid and given by

$$g(z, z_0) = -\ln(z - \bar{z}_0) - \frac{1 - ij}{(1-4\tau)^{\frac{1}{2}}}[F_1(z, z_0) - F_2(z, z_0)] - \frac{1 + ij}{(1+4\tau)^{\frac{1}{2}}}[F_3(z, z_0) - F_4(z, z_0)]. \tag{3.3}$$

Here
$$F_n(z, z_0) = \exp(-ik_n z) \int_{C_n}^{z} \frac{\exp(ik_n u)}{u - \bar{z}_0} du \quad (n = 1, 2, 3, 4). \tag{3.4}$$

A bar denotes the complex conjugate, and C_n is defined by

$$\left.\begin{aligned} &C_n = \infty \quad (n = 1, 3, 4), \quad C_2 = -\infty \quad (\tau < \tfrac{1}{2}), \\ &C_n = i\infty/k_n \quad (n = 1, 2), \quad C_n = \infty \ (n = 3, 4) \quad (\tau > \tfrac{1}{2}). \end{aligned}\right\} \tag{3.5}$$

Furthermore
$$\left.\begin{aligned} k_{1,2} &= \frac{\nu}{2\tau^2}[1 - 2\tau \pm (1-4\tau)^{\frac{1}{2}}], \\ k_{3,4} &= \frac{\nu}{2\tau^2}[1 + 2\tau \pm (1+4\tau)^{\frac{1}{2}}], \end{aligned}\right\} \tag{3.6}$$

where
$$\nu = \frac{\sigma^2}{g}, \quad \tau = \frac{U\sigma}{g}. \tag{3.7}$$

The function $f_1(z)$, given by (3.1), satisfies for every γ all boundary conditions except the kinematic boundary condition at the body (2.7) and the Kutta condition at the trailing edge.

To determine γ such that these two conditions are also fulfilled we first introduce the velocities u and v, defined by

$$u - iv = \frac{df}{dz} = \frac{df_0}{dz} + \frac{df_1}{dz}, \tag{3.8}$$

where we have applied (2.13). It is seen from (2.10) that u and v are related to the real velocity by

$$\left.\begin{aligned} \frac{\partial \phi}{\partial x} &= \mathrm{Re}_j\, u \exp(j\sigma t), \\ \frac{\partial \phi}{\partial y} &= \mathrm{Re}_j\, v \exp(j\sigma t). \end{aligned}\right\} \tag{3.9}$$

Introducing (3.1) into (3.8) we obtain

$$u - iv = \frac{df}{dz} = \frac{df_0}{dz} + \int_{-\infty}^{l} \gamma(\xi) \frac{\partial G}{\partial z}(z, \xi - id)\, d\xi. \tag{3.10}$$

To apply the boundary condition at the foil, we let $z \to x - id$ from below and above. The Plemelj formula then gives

$$u - iv = \frac{df_0}{dz} + \int_{-\infty}^{l} \gamma(\xi) \frac{\partial G}{\partial z}(z, \xi - id)\, d\xi \pm \tfrac{1}{2}\gamma(x) \quad (z = x - id, x < l). \tag{3.11}$$

Here ' + ' and ' − ' correspond to $z \to x - id$ from below and above, respectively, and the bar through the integral sign indicates the principal value.

Equation (3.11) contains two equations. Since the velocity circulation around the foil is non-zero, u has different values on the upper and lower side of the foil. v, on the other hand, has the same value on both sides. Substracting the two equations in (3.11) from each other, we find that

$$\gamma = \Delta u, \tag{3.12}$$

where Δ denotes the difference between the lower and upper value along the cut $-\infty < x < l$, $y = -d$.

Equation (3.12) identifies the physical meaning of γ, but does not help us to calculate the value since Δu is unknown. An equation for determining γ is obtained by taking the imaginary part with respect to i of (3.11) for $|x| < l$. This gives

$$-v = \mathrm{Im_i}\frac{\mathrm{d}f_0}{\mathrm{d}z} + \int_{-\infty}^{l} \gamma(\xi)\,\mathrm{Im_i}\frac{\partial G}{\partial z}(z, \xi - \mathrm{i}d)\,\mathrm{d}\xi \quad (z = x - \mathrm{i}d),\ |x| < l). \tag{3.13}$$

For $|x| < l$, v is known from the boundary condition (2.5) and (3.9) where ζ is known. We see that

$$\mathrm{Re_j}\, v \exp(\mathrm{j}\sigma t) = \left(\frac{\partial}{\partial t} - U\frac{\partial}{\partial x}\right)\zeta. \tag{3.14}$$

Since (3.13) is only valid for $|x| < l$ and γ is unknown in the interval $< -\infty, -l >$, additional information about γ is needed. This is obtained by noting that the vorticity in the wake is conserved. Hence,

$$\left(\frac{\partial}{\partial t} - U\frac{\partial}{\partial x}\right)\Delta\frac{\partial \phi}{\partial x} = 0 \quad (-\infty < x < -l), \tag{3.15}$$

which has the solution

$$\Delta\frac{\partial \phi}{\partial x}(x, t) = \Delta\frac{\partial \phi}{\partial x}(x + Ut) \quad (-\infty < x < -l). \tag{3.16}$$

From (3.9) and (3.12)

$$\gamma = \gamma_0 \exp(\mathrm{j}kx) \quad (-\infty < x < -l), \tag{3.17}$$

where γ_0 is complex with respect to j. k is the reduced frequency given by

$$k = \sigma / U; \tag{3.18}$$

γ is therefore known in the wake, except for the amplitude γ_0. To obtain γ_0 we set the amount of vorticity which is shed at the trailing edge per unit time, $-U\mathrm{Re_j}\,\gamma(-l)$ $\exp(\mathrm{j}\sigma t)$, equal to the rate of change of the velocity circulation around the foil. Let Γ be defined by

$$\Gamma = \int_{-l}^{l} \gamma \mathrm{d}\xi. \tag{3.19}$$

We then have, according to (3.9), (3.12) and (3.17),

$$\mathrm{j}\sigma\Gamma = -U\gamma(-l) = -U\gamma_0 \exp(-\mathrm{j}kl), \tag{3.20}$$

(3.20) associates γ_0 with Γ. The latter will be found by applying the Kutta condition at the trailing edge.

Considering for the moment γ_0 as known and applying (3.17), (3.13) is a singular integral equation of the first kind which determines γ in the interval $< -l, l >$. This

integral equation may easily be transformed to a Fredholm equation of the second kind, which is convenient for numerical solution. This is obtained by writing (3.13) in the form

$$\int_{-l}^{l} \frac{\gamma(\xi)}{x-\xi} \mathrm{d}\xi = -H(x) - F(x), \tag{3.21}$$

where
$$H(x) = -2\pi \mathrm{Im}_{\mathrm{i}} \frac{\mathrm{d}f_0}{\mathrm{d}z} - 2\pi v \quad (z = x - \mathrm{i}d), \tag{3.22}$$

and
$$F(x) = \gamma_0 \int_{-\infty}^{-l} \exp(\mathrm{j}k\xi) \left[\frac{1}{x-\xi} - K(x,\xi)\right] \mathrm{d}\xi - \int_{-l}^{l} \gamma(\xi) K(x,\xi) \mathrm{d}\xi, \tag{3.23}$$

with
$$K(x,\xi) = \mathrm{Re}_{\mathrm{i}} \frac{\partial g}{\partial z}(z, \xi - \mathrm{i}d) \quad (z = x - \mathrm{i}d). \tag{3.24}$$

If the foil is sufficiently deeply submerged, $K(x,\xi)$ may be neglected. The equation then describes the unsteady hydrofoil problem in an unbounded fluid. Considering for the moment the right-hand side of (3.21) as known, the solution of the equation is (see Newman 1977, p. 182)

$$\gamma(x) = \frac{1}{\pi^2} (l^2 - x^2)^{-\frac{1}{2}} \left[\int_{-l}^{l} \frac{(l^2-\eta^2)^{\frac{1}{2}}}{x-\eta} (H(\eta) + F(\eta)) \mathrm{d}\eta + \pi\Gamma \right]. \tag{3.25}$$

From residue calculation we obtain

$$\int_{-l}^{l} \frac{(l^2-\eta^2)^{\frac{1}{2}}}{(x-\eta)(\eta-\xi)} \mathrm{d}\eta = \pi - \frac{\pi}{x-\xi} (\xi^2 - l^2)^{\frac{1}{2}} \quad (\xi < -l, |x| < l). \tag{3.26}$$

By using (3.26) and (3.20) we find after some algebra that (3.25) may be written in the form

$$\kappa(x) + \int_{-l}^{l} \kappa(\xi) \frac{\tilde{K}(x,\xi)}{(l^2-\xi^2)^{\frac{1}{2}}} \mathrm{d}\xi = \tilde{H}(x) + \gamma_0 P(x). \tag{3.27}$$

Here the tilde defines the transform

$$\tilde{f}(x) = \frac{1}{\pi^2} \int_{-l}^{l} \frac{(l^2-\eta^2)^{\frac{1}{2}}}{x-\eta} f(\eta) \mathrm{d}\eta. \tag{3.28}$$

Furthermore,
$$\kappa(x) = (l^2 - x^2)^{\frac{1}{2}} \gamma(x), \tag{3.29}$$

and
$$P(x) = -\int_{-\infty}^{-l} \exp(\mathrm{j}k\xi) \left[\frac{\mathrm{j}}{k\pi} \frac{\mathrm{d}}{\mathrm{d}\xi} \left(\frac{(\xi^2-l^2)^{\frac{1}{2}}}{x-\xi} \right) + \tilde{K}(x,\xi) \right] \mathrm{d}\xi. \tag{3.30}$$

For numerical purpose $P(x)$ may be considerably simplified, see Appendix A.

To close the problem we apply the Kutta condition at the trailing edge. Requiring $\gamma(-l)$ to be finite, and applying (3.27) and (3.29), we find

$$\gamma_0 = \left[\int_{-l}^{l} \kappa(\xi) \frac{\tilde{K}(-l,\xi)}{(l^2-\xi^2)^{\frac{1}{2}}} \mathrm{d}\xi - \tilde{H}(-l) \right] \frac{1}{P(-l)}. \tag{3.31}$$

Replacing γ_0 in (3.27) with (3.31) we finally obtain

$$\kappa(x) + \int_{-l}^{l} \kappa(\xi) \frac{\tilde{K}(x,\xi) - \tilde{K}(-l,\xi) P(x)/P(-l)}{(l^2-\xi^2)^{\frac{1}{2}}} \mathrm{d}\xi = \tilde{H}(x) - \tilde{H}(-l) P(x)/P(-l), \tag{3.32}$$

which is the governing integral equation for the problem.

It may be worth mentioning that in the derivation of (3.27) we have – in opposition to what seems to be standard in similar derivations in related problems – brought the infinite integrals on a form which imply that they exist in the ordinary sense, without any artificial viscosity. This is obtained by applying Kelvin's theorem in the form (3.20) and not splitting the two terms on the right-hand side of (3.26).

4. Numerical solution

The integral equation (3.32) is solved by a collocation method. New variables are introduced by

$$x = l\cos t, \quad \xi = l\cos s, \quad \eta = l\cos r \quad (t, s, r \in <0, \pi>).$$

The t-interval $<0, \pi>$ is subdivided into N equal segments. In this manner a fine subdivision is obtained close to the leading and trailing edges where variations in κ are stronger than at the middle of the chord. The unknown κ is assumed constant at each segment. A set of $N \times N$ equations is then obtained by fulfilling the integral equation at the points $t_n = (n-\frac{1}{2})\pi/N$, $n = 1, 2, \ldots, N$. The integrals of the kernel over each segment are calculated by applying two-point Gauss quadrature. Since any symmetric integration rule may be applied to the principal value integral (3.28), even with the substitution $x = l\cos t$, $\xi = l\cos s$, we also calculate this integral by two-points Gauss quadrature. In all calculations presented $N = 25$ is applied, giving an accuracy of 1% or better. As a check of the computations the wasted energy is calculated by (5.6) and by far-field analysis (5.17).

5. Discussion of the results. No incoming waves

We assume no incoming waves in this section. The foil is performing a heaving motion with amplitude h, a pitching motion with maximum angle α and there may be an arbitrary phase between these two motions. Instead of using these three parameters we find it appropriate to follow Lighthill (1970) in writing the vertical displacement of the foil in the form

$$\zeta(x,t) = \mathrm{Re}_{\mathrm{j}}[h + \mathrm{j}\alpha(x-b)]\exp(\mathrm{j}\sigma t). \tag{5.1}$$

In this notation $x = b$ is the location of the pitch axis and h denotes the (positive) heave amplitude of the pitch axis. α denotes, as above, the maximum angle of the pitch motion and may be positive or negative. In this representation the heaving and pitching has a specified phase lag of 90°, whereas the location of the pitch axis is unknown.

The oscillating foil will generate surface waves with frequency σ. At large distances from the oscillating foil the waves will be sinusoidal waves with wavenumbers k_1, k_2, k_3, k_4 defined by (3.6) (for a discussion of the waves, see for example Grue & Palm 1985). For $\tau = U\sigma/g$ less than $\frac{1}{4}$, all four waves will be generated, for τ larger than $\frac{1}{4}$ only the k_3 wave and k_4 wave will be generated. The k_1 wave and k_2 wave have positive phase velocities. The k_2 wave has also positive group velocity whereas the k_1 wave has negative group velocity. The k_2 wave will therefore be located upstream and the k_1 wave downstream. The k_3 wave and the k_4 wave have negative phase and group velocities, and are located downstream. The phase velocity of the k_3 wave is less than U whereas the phase velocity of the k_4 wave is larger than U. In the frame of reference where the current is zero, both the k_1 wave and the k_2 wave have positive phase velocities larger than U. The k_1 wave has group velocity less than U whereas

the k_2 wave has group velocity larger than U. The k_3 wave has positive phase velocity smaller than U, and the k_4 wave has negative phase velocity.

The wave elevation at $x = \pm\infty$ will be composed of waves of the form

$$\mathrm{Re_j}\, a_n \exp(\mp \mathrm{j}k_n x + \mathrm{j}\sigma t) \quad (n = 1, 2, 3, 4). \tag{5.2}$$

The amplitudes a_n are derived in Appendix B and are found to be

$$a_n = \left(\frac{k_n/g}{1-4\tau}\right)^{\frac{1}{2}} \exp(-k_n d) \int_{-l}^{l} \left[\exp(\mathrm{j}k_n x) - \frac{k}{k+k_n} \exp(-\mathrm{j}k_n l)\right] \gamma(x)\, \mathrm{d}x \quad (n = 1, 2), \tag{5.3}$$

and

$$a_n = \left(\frac{k_n/g}{1+4\tau}\right)^{\frac{1}{2}} \exp(-k_n d) \int_{-l}^{l} \left[\exp(\mathrm{j}k_n x) - \frac{k}{k-k_n} \exp(-\mathrm{j}k_n l)\right] \overline{\gamma(x)}\, \mathrm{d}x \quad (n = 3, 4). \tag{5.4}$$

For $\tau > \frac{1}{4}$, both a_1 and a_2 are zero. Apparently a_1 and a_2 tend towards infinity as $\tau \to \frac{1}{4}$. It may be argued and the numerical solutions show, however, that a_1 and a_2 tend towards a finite limit as $\tau \to \frac{1}{4}$. The same result was found for a submerged circular cylinder by Grue & Palm (1985) and for a submerged elliptic cylinder by Mo & Palm (1987).

In the discussion of the results and comparison with experiments we shall apply the energy equation in the frame of reference where the current is zero (the foil moving with velocity U). To maintain the prescribed motion there must be an external force providing the necessary rate of work, the power. The mean power P is here given by

$$P = -\overline{\int_{-l}^{l} \Delta p \frac{\partial \zeta}{\partial t}\, \mathrm{d}x}, \tag{5.5}$$

where Δp is the pressure difference between the lower and upper side, and the bar denotes time average. The energy equation, averaged in time, may be written

$$P = TU + E. \tag{5.6}$$

Here T is the mean thrust acting upon the foil in the x-direction, and E is the mean wasted energy due to the wake and the scattering of surface waves.

It is of interest to note that the mean thrust is composed of two terms, here denoted by $\bar{T}_\mathrm{s}$ and $\bar{T}_\mathrm{p}$ so that

$$T = \bar{T}_\mathrm{s} + \bar{T}_\mathrm{p}. \tag{5.7}$$

T_s is a suction force acting at the leading edge and is due to the fact that the velocity in our model here is infinite. In a more realistic model with a rounded leading edge the velocity will be finite, but fast. Also in this model there is a suction force, given approximately by (5.10). The suction force may be found by applying Blasius formula to a small circle of radius ϵ surrounding the leading edge. The suction force is then given by

$$T_\mathrm{s} = \mathrm{Re_i}\, \tfrac{1}{2}\mathrm{i}\rho \oint_{\epsilon} [\mathrm{Re_j}(f_1'(z) \exp(\mathrm{j}\sigma t))]^2\, \mathrm{d}z, \tag{5.8}$$

where ρ is density and $f_1(z)$ is given by (3.1). Only the part of $f_1'(z)$ which is singular for $z \to l$, gives contribution to (5.8). We find that

$$f_1'(z) = \frac{\kappa(l)}{2i(2l)^{\frac{1}{2}}}(z-l)^{-\frac{1}{2}} + O(1). \tag{5.9}$$

Introducing (5.9) into (5.8) gives

$$T_s = \frac{\pi\rho}{8l}[\mathrm{Re}_j(\kappa(l)\exp(j\sigma t))]^2. \tag{5.10}$$

The other term $\bar{T}_p$ is due to the pressure difference along the foil and may be called the sideforce. T_p is given by

$$T_p = \int_{-l}^{l} \Delta p \frac{\partial \eta}{\partial x} \mathrm{d}x. \tag{5.11}$$

Introducing the notation

$$L = \int_{-l}^{l} \Delta p \, \mathrm{d}x, \tag{5.12}$$

where L is the pressure force perpendicular to the plate, we have

$$T_p = L\frac{\partial \eta}{\partial x}. \tag{5.13}$$

To obtain a formula for the last term in (5.6), the mean wasted energy, we first consider the waste due to the wake. This waste is manifested by the wake being increased a length per unit time equal to U. The mean wasted energy is therefore equal to the energy density of the vortex wake multiplied by U. The velocity field generated by the wake (in the frame of reference where the foil moves with speed U) is given by

$$\phi_1(x,y) = -\frac{|\gamma_0|}{k}\exp(-kd)\cosh(ky)\sin(kx + \arg\gamma_0) \quad (y > -d), \tag{5.14}$$

$$\phi_1(x,y) = \frac{|\gamma_0|}{k}\sinh(kd)\exp(ky)\sin(kx + \arg\gamma_0) \quad (y < -d), \tag{5.15}$$

(5.14) and (5.15) lead to a mean waste of energy equal to

$$\frac{1}{8k}\rho U|\gamma_0|^2[1-\exp(-2kd)]. \tag{5.16}$$

Correspondingly, the generated wave trains are increased a length per unit time equal to $|c_{gn}-U|$ $(n = 1, 2, 3, 4)$ where c_{gn} is the group velocity. The mean waste of energy per unit time due to the waves is therefore equal to $|c_{gn}-U|E_n$ where E_n $(n = 1, 2, 3, 4)$ is the wave energy density. We thus obtain

$$E = E_2|c_{g2}-U| + E_1|c_{g1}-U| + E_3|c_{g3}-U| + E_4|c_{g4}-U| + \frac{1}{8k}\rho U|\gamma_0|^2[1-\exp(-2kd)], \tag{5.17}$$

with

$$E_n = \tfrac{1}{2}\rho g|a_n|^2 \quad (n = 1, 2, 3, 4), \tag{5.18}$$

and

$$\left.\begin{aligned} c_{gn} &= \tfrac{1}{2}c_n = \tfrac{1}{2}(g/k_n)^{\frac{1}{2}} \quad (n = 1, 2, 3), \\ c_{g4} &= \tfrac{1}{2}c_4 = -\tfrac{1}{2}(g/k_4)^{\frac{1}{2}} \end{aligned}\right\} \tag{5.19}$$

It is seen from (5.14) that the effect of the wake is not felt directly at the free surface since the vertical velocity as well as the pressure due to the wake here is zero. We also mention that the wavenumber k in the wake is never equal to k_n ($n = 1, 2, 3, 4$), except for the singular case $\tau = \frac{1}{4}$. We therefore obtain no kind of resonance between the periodic wake and the waves.

Corresponding to the wave energy loss, there is change in the momentum due to the waves. This change of momentum per unit time leads to a thrust on the foil, T_w. The contributions from the various waves are obtained by dividing the respective energy losses with the phase velocity (see for example equation (4.24) in Grue & Palm 1985). T_w is given by

$$T_w = -\frac{E_2}{c_2}|c_{g2}-U| - \frac{E_1}{c_1}|c_{g1}-U| - \frac{E_3}{c_3}|c_{g3}-U| - \frac{E_4}{c_4}|c_{g4}-U|. \tag{5.20}$$

It is seen that the k_1 wave, the k_2 wave and the k_3 wave which all propagate in the positive x-direction, give rise to a negative thrust. The k_4 wave which propagates in the negative x-direction, contributes to a positive thrust. The total thrust is composed of T_w and the thrust due to the wake. The latter seems, however, impossible to evaluate directly.

In displaying our results it is appropriate to give the thrust, for example, in the non-dimensional form $T/\rho g h^2$. This dimensionless thrust depends on five dimensionless parameters which may be chosen as d/l, $U/(gl)^{\frac{1}{2}}$, b/l, $\sigma^2 l/g$, $\alpha U/\sigma h$. Here $U/(gl)^{\frac{1}{2}}$ is a Froude number and will be denoted by Fr. The parameter $\alpha U/\sigma h$ provides a measure of the relative magnitude of pitch and heave and is denoted as the feathering parameter θ by Lighthill (1970). We have

$$\theta = \frac{\alpha U}{\sigma h} = \frac{\alpha}{\alpha_0}, \quad \alpha_0 = \frac{\sigma h}{U}. \tag{5.21}$$

It is noted from (5.1) that θ is the ratio between the instantaneous pitch angle $-\alpha \sin \sigma t$ and the instantaneous gliding angle $-\alpha_0 \sin \sigma t$. For low frequencies and the foil deeply submerged, the total force on the foil from the fluid is equal to the lift. In this case we obtain negative thrust if the pitch angle is larger than the gliding angle, i.e. $\theta > 1$. This motivates us to consider only values of θ smaller than unity. In the analysis we have assumed that stall does not occur. There is, in general, no simple criterion for deciding whether or not stall occurs for an oscillating foil. However, for small frequencies, the instantaneous angle of attack, which reads

$$-\alpha_0 \sin \sigma t + \alpha \sin \sigma t = -\alpha_0 (1-\theta) \sin \sigma t, \tag{5.22}$$

must be small for avoiding stall. Also, if the foil is deeply submerged, it is easily found that

$$\frac{\bar{T}_s}{T} = \frac{\alpha_0 - \alpha}{\alpha_0}. \tag{5.23}$$

Hence, stall is avoided if either α_0 is small or $\bar{T}_s/T$ is small. For higher values of σ Lighthill (1970) has suggested that stall may occur if T_s is too large compared with the total value of T. This will happen if the sideforce is large and gives a negative contribution to the thrust. In displaying our results we shall therefore try to avoid values of the parameter leading to such values of the sideforce, and also in some cases give the value of $\bar{T}_s$ together with T.

With as many as five non-dimensional parameters in the problem, space limitations only permit us to display the results of some few values of each parameter. In the comparison with experiments in §7 we have of course to choose the values used in the

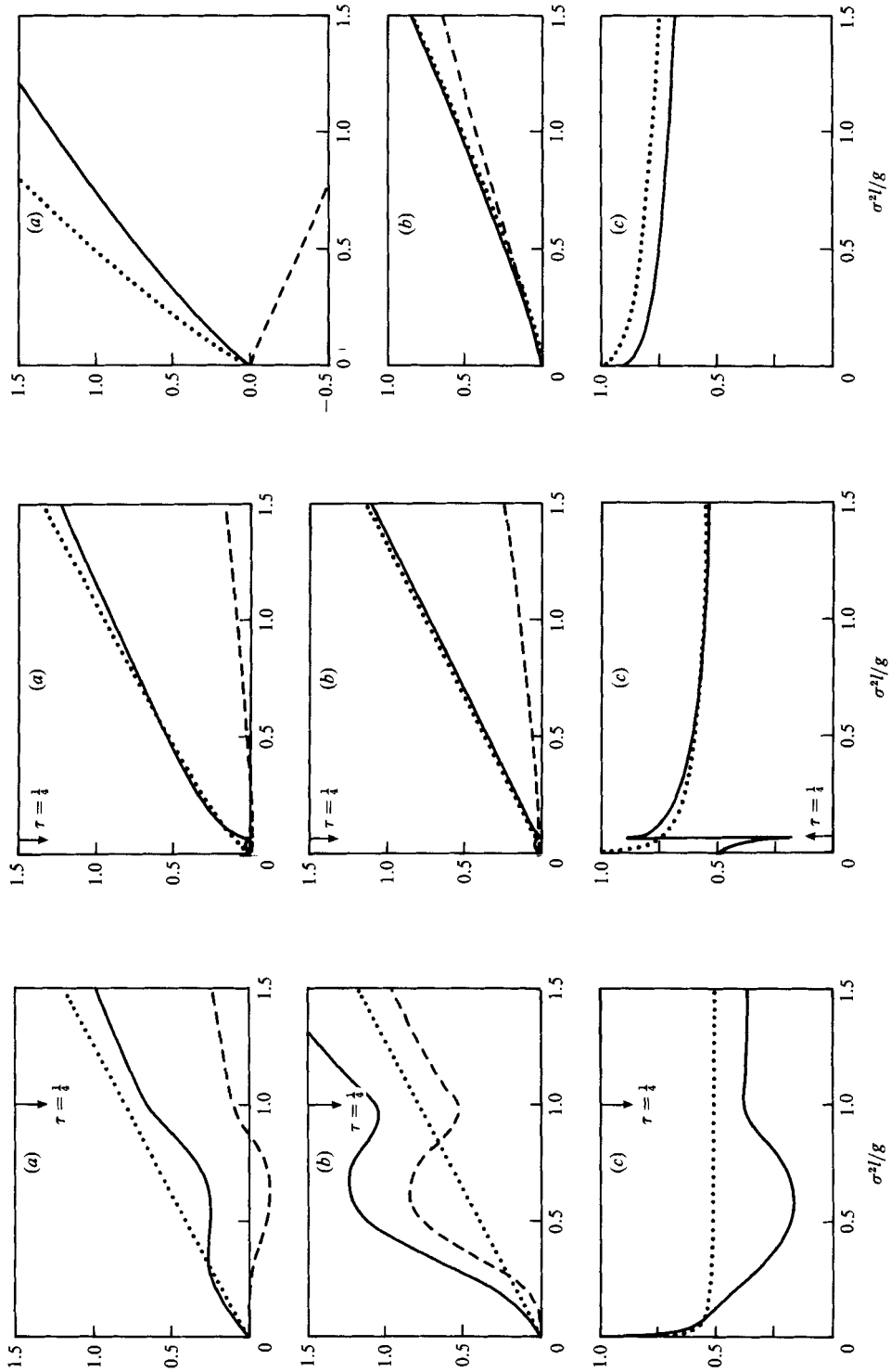

FIGURE 2. $Fr = 0.25$.

FIGURE 3. $Fr = 1$.

FIGURE 4. $Fr = 5$.

FIGURES 2–4. Values of thrust, energy waste and efficiency *vs.* $\sigma^2 l/g$. Foil oscillating in heaving motion in calm water. $d/l = 1$, $\theta = 0$. (*a*) ——, $T/\rho g h^2$; – – –, $T_w/\rho g h^2$; ···, $T/\rho g h^2$ for $d = \infty$. (*b*) ——, $E/\rho g h^2 U$; – · –, $E_w/\rho g h^2 U$; ···, $E/\rho g h^2 U$ for $d = \infty$. (*c*) ——, TU/P for $d/l = 1$; ···, TU/P for $d = \infty$.

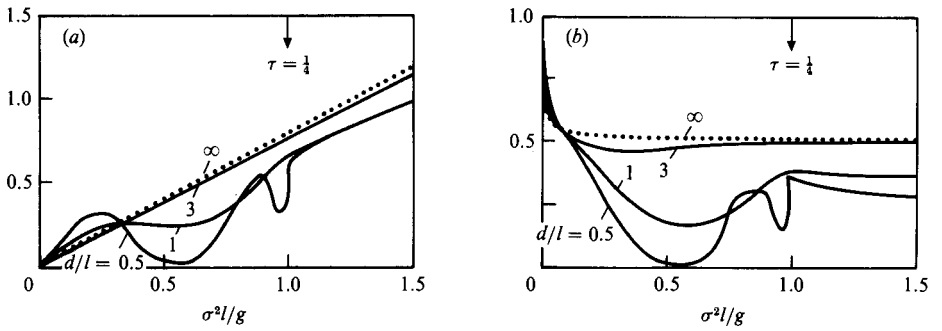

FIGURE 5. Values of thrust and efficiency *vs.* $\sigma^2 l/g$ for various values of submergence of the foil. Foil oscillating in heaving motion in calm water. $Fr = 0.25$, $\theta = 0$, $d/l = 0.5, 1, 3, \infty$. (*a*) $T/\rho g h^2$, (*b*) TU/P.

experiments. In §§5 and 6 we have chosen $d/l = 0.5, 1, 3, \infty$ and $Fr = 0.25, 1, 5$. Furthermore, θ is given the values $\theta = 0$ and $\theta = 0.6$. $\theta = 0$ usually gives a large thrust, but small efficiency. $\theta = 0.6$ gives in general smaller thrust, but considerably higher efficiency. b/l is chosen as -0.5, 0 or 0.5. Smaller values of b/l give very high values of T_s/T.

The figures are displayed with $\sigma^2 l/g$ as abscissa which varies from 0 to 1.5. For larger values of $\sigma^2 l/g$ the variation of the thrust and wasted energy is rather monotonous. In figures 2, 3, 4 and 5, θ is zero, i.e. the foil is performing a pure heaving motion. It is seen from the figures that the effect of the generated waves are important. Thus the energy waste due to the waves, E_w, may be the dominant part of the waste. We note that E_w is about 60% of the total energy waste for $Fr = 0.25$ and almost the total energy waste for $Fr = 5$. The thrust due to the waves, T_w, is found to be negative for $\tau < \frac{1}{4}$ since the k_1 and k_2 waves then are the dominating waves. T_w becomes, however, positive when the k_4 wave is the most pronounced of the radiated waves which occurs for $\tau > \frac{1}{4}$, and small and moderate values of the Froude number, as seen in figures 2 and 3. For larger Froude numbers the k_3 wave is the dominating one and T_w becomes negative, as shown in figure 4. A remarkable feature for the energy waste is shown in figures 3 and 4 for $Fr = 1$ and 5, respectively. It is seen that the curves for the energy waste are almost identical for $d/l = 1$ and $d/l = \infty$, in spite of the fact that the energy waste due to the waves is significant for $d/l = 1$. This paradox is most pronounced for $Fr = 5$ where for $d/l = 1$ the energy waste due to the waves is indeed by far the most important part of the total energy waste.

The effect of the submergence of the foil is shown in figure 5 for $Fr = 0.25$. We notice that the thrust and efficiency have local maxima when the foil is sited very close to the free surface and τ is slightly smaller than $\frac{1}{4}$. This is due to a resonance phenomena being discussed in §7.

In figures 6, 7, 8 and 9 the effect of a pitching motion, with $\theta = 0.6$, is shown. For $Fr = 0.25$ we find that the pitching motion produces both a larger thrust and a larger efficiency, than obtained for $\theta = 0$. For larger Froude numbers the pitching motion reduces the thrust but increases the efficiency. The effect of the free surface is less pronounced for $\theta = 0.6$ than for $\theta = 0$. The scattered surface waves are much smaller in this case, but cannot be neglected. In figure 9 the effect of choosing different values for the locaion of the pitching axis is examined. We see that for $Fr = 0.25$ and $b/l = 0.5$, $\bar{T}_s/T \ll 1$. Also for $b/l = 0$, $\bar{T}_s/T < 1$. For $b/l = -0.5$, however, we find that

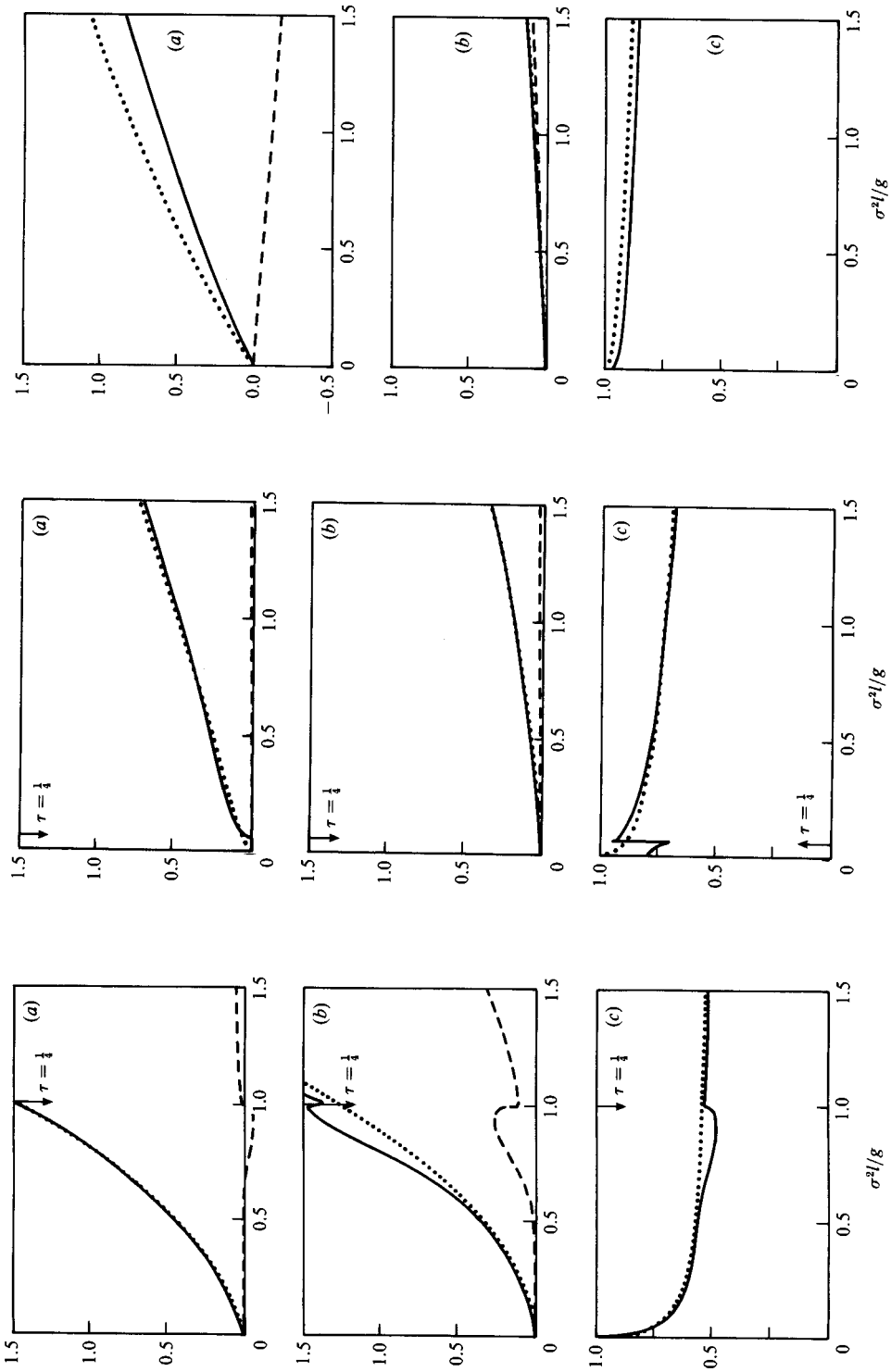

FIGURE 6. $Fr = 0.25$.

FIGURE 7. $Fr = 1$.

FIGURE 8. $Fr = 5$.

FIGURES 6–8. Same as figures 2–4, but foil oscillating in heaving and pitching motions in calm water, $\theta = 0.6$, $b/l = 0$.

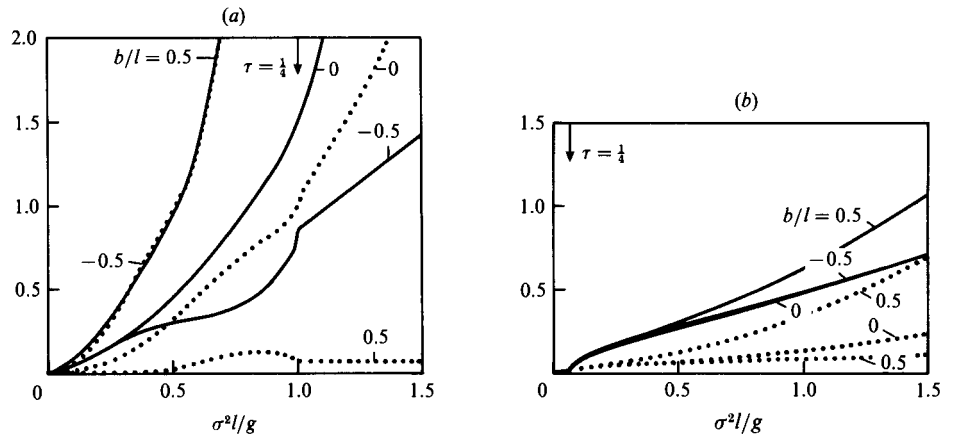

FIGURE 9. Values of thrust *vs.* $\sigma^2 l/g$ for various values of pitch axis. Foil moving in heaving and pitching motions in calm water. ——, $T/\rho g h^2$; ···, $\bar{T}_s/\rho g h^2$. $\theta = 0.6$, $b/l = -0.5, 0, 0.5$ (*a*) $Fr = 0.25$, (*b*) $Fr = 1$.

$\bar{T}_s/T \gg 1$ for moderate values of $\sigma^2 l/g$. This suggests that for negative values of b/l, the possibility for stall is large for small Froude numbers. For $Fr = 1$, $T_s/T < 1$ for all shown values of $\sigma^2 l/g$. Similar results were obtained by Lighthill (1970) for a foil oscillating in an unbounded fluid.

6. Discussion of the results. Incoming waves

6.1. *General*

We consider next a foil oscillating in incoming waves. The frequency of encounter of the waves equals the frequency σ of the foil motion. The incoming wave elevation may then be written

$$\eta_0 = a_0 \sin(k_0 x \pm \sigma t), \tag{6.1}$$

where a_0 is the wave amplitude and k_0 the wavenumber. The arbitrary phase angle between the wave and the foil oscillation will be taken into account in the expression for the foil oscillation (6.5). Furthermore, the + sign is applied for $k_0 = k_3, k_4$ and the − sign for $k_0 = k_1, k_2$. The complex velocity potential corresponding to η_0 reads

$$f_0(z) = \delta a_0 \left(\frac{g}{k_0}\right)^{\frac{1}{2}} (1 \pm \mathrm{ij}) \exp(-\mathrm{i}k_0 z), \tag{6.2}$$

where $\delta = -1$ for $k_0 = k_1, k_2, k_3$ and $\delta = 1$ for $k_0 = k_4$. The former waves are travelling in the positive x-direction in the fixed frame of reference (in which the foil is moving with velocity U) and will be called following waves. The latter wave is in this frame of reference moving in the negative x-direction and will be denoted as the head wave. An incoming following wave is a k_2 wave if $0 < k_0 < 0.25 g/U^2$, a k_1 wave if $0.25 g/U^2 < k_0 < g/U^2$, or a k_3 wave if $k_0 > g/U^2$. The incoming wave will be transmitted by the foil. In addition, three new waves are set up for $\tau < \frac{1}{4}$, and for $\tau > \frac{1}{4}$ one new wave is generated.

The energy equation is readily obtained from (5.6) and (5.17) by adding the energy contribution from the incoming wave, P_0, say, on the left-hand side. The energy equation then takes the form

$$P + P_0 = TU + E. \tag{6.3}$$

By the same reasoning as in §5, we find that

$$P_0 = E_0 |c_g - U|, \tag{6.4}$$

where $E_0 = \frac{1}{2}\rho g a_0^2$, $c_g = -\frac{1}{2}(g/k_0)^{\frac{1}{2}}$ for the head wave (k_4 wave) and $c_g = \frac{1}{2}(g/k_0)^{\frac{1}{2}}$ for following waves (k_1, k_2, k_3 wave). It is noted that for given P (for example $P = 0$), (6.3) gives the thrust T by the far-field quantities alone. We have not succeeded in obtaining a similar expression for T by applying the momentum equation.

The effect of long incoming waves, i.e. waves for which $k_0 l \ll 1$, is essentially only to introduce an extra heave motion, also when the heave oscillation of the foil and the wave motion are completely out of phase. To see this we rewrite the expression for the foil motion in a form slightly different to (5.1)

$$\zeta(x,t) = \mathrm{Re}_{\mathrm{j}}[h + \mathrm{j}\alpha(x-b)\exp(\mathrm{j}\chi)]\exp(\mathrm{j}\sigma t + \mathrm{j}\psi). \tag{6.5}$$

Here ψ is the arbitrary phase angle between the heave motion of the foil and the wave motion. χ is a not yet specified angle. If χ is different from zero, we see that in the representation (6.5) the heave and pitch motions are not 90° out of phase, as was the case in the form (5.1). The right-hand side of the governing integral equation (3.32) is only dependent on the value of the vertical velocity $\partial\phi_1/\partial y$ at the foil (see (3.22), (3.14) and (2.7)). We obtain from (2.7), (6.5), (6.2) and (2.12) that

$$\frac{\partial\phi_1}{\partial y} = \mathrm{Re}_{\mathrm{j}}\left\{j\sigma\left[h + \left(-\frac{U\alpha}{\sigma} + \mathrm{j}\alpha(x-b)\right)\exp(\mathrm{j}\chi) + \mathrm{j}\hat{a}_0\delta\exp(\pm\mathrm{j}k_0 x - \mathrm{j}\psi)\right]\exp(\mathrm{j}\sigma t + \mathrm{j}\psi)\right\}, \tag{6.6}$$

where

$$\hat{a}_0 = a_0\frac{\omega}{\sigma}\exp(-k_0 d). \tag{6.7}$$

For $k_0 l \ll 1$, we may replace $\exp(\pm\mathrm{j}k_0 x)$ with 1. Furthermore, we introduce $\hat{h}$ and $\hat{\psi}$ defined by

$$h + \mathrm{j}\hat{a}_0\delta\exp(-\mathrm{j}\psi) = \hat{h}\exp(\mathrm{j}\hat{\psi}), \tag{6.8}$$

with

$$\hat{h} = (h^2 + \hat{a}_0^2 + 2h\hat{a}_0\delta\sin\psi)^{\frac{1}{2}}. \tag{6.9}$$

Now specifiying χ by

$$\chi = \hat{\psi}, \tag{6.10}$$

we find that for long incoming waves the boundary condition at the foil is

$$\frac{\partial\phi_1}{\partial y} = \mathrm{Re}_{\mathrm{j}}\left\{\mathrm{j}\sigma\left(\hat{h} - \frac{U\alpha}{\sigma} + \mathrm{j}\alpha(x-b)\right)\exp(\mathrm{j}\hat{\psi} + \mathrm{j}\psi + \mathrm{j}\sigma t)\right\}. \tag{6.11}$$

Replacing $\hat{h}$ with h (6.11) is, apart from an unimportant time phase $\hat{\psi} + \psi$, identical to the vertical velocity obtained from (5.1). We thus find that the two motions represented by (5.1) and (6.11) have, according to (3.32) the same values of κ. A straightforward generalization of the feathering parameter defined in §5 is now

$$\hat{\theta} = \alpha U/\sigma\hat{h}, \tag{6.12}$$

being valid also for long incoming waves. We notice that the effect of long waves is to change h to $\hat{h}$ and the feathering parameter to the form (6.12). The location of the pitch axis, given by b, is however not changed. The definition (6.12) of the feathering parameter for incoming waves is quite different from the definition given by Wu (1972).

We may now conclude that $T/\rho g\hat{h}^2$ is independent of $\hat{a}_0/h$ and the phase angle ψ for long incoming waves. In other words, the thrust may in this case be obtained

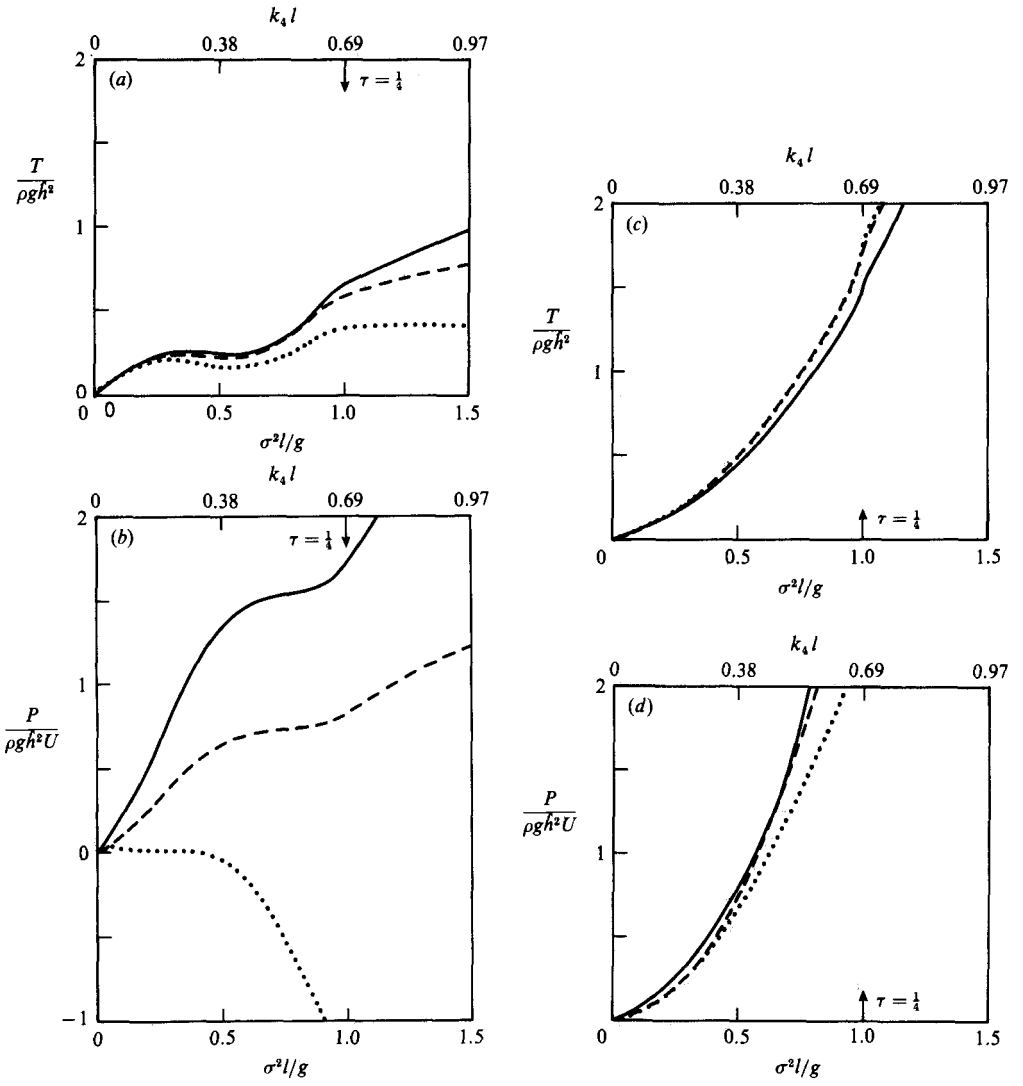

FIGURE 10. Values of thrust $T/\rho g\hat{h}^2$ and power $P/\rho g\hat{h}^2 U$ *vs.* $\sigma^2 l/g$. ——, foil oscillating in calm water. – – –, foil oscillating in incoming head waves, 180° out of phase with the wave motion ($\psi = \frac{1}{2}\pi$) and $a_0/h = 1$. ···, foil oscillating in incoming head waves, 90° out of phase with the wave motion ($\psi = 0$) and $\hat{a}_0/h = 1$, $d/l = 1$, $Fr = 0.25$. (*a*) and (*b*): $\hat{\theta} = 0$, (*c*) and (*d*): $\hat{\theta} = 0.6$, $b/l = 0$.

by studying the oscillation of a foil in calm water by applying the same values of $\hat{h}$ and $\hat{\theta}$ in the two cases. The same conclusion is obviously not true for the power $P/\rho g h^2 U$. To examine the behaviour of the thrust and power more closely we display in figure 10 $T/\rho g\hat{h}^2$ and $P/\rho g\hat{h}^2 U$ as functions of $\sigma^2 l/g$ without making any assumption as to the wavelength of the incoming wave. The thrust and power for the foil oscillating in calm water and the foil oscillating in incoming head waves are shown in the figures. The latter are either 180° or 90° out of phase with the foil oscillation, corresponding to $\psi = \frac{1}{2}\pi$ and $\psi = 0$, respectively. $\hat{a}_0/h = 1$, $\theta = 0, 0.6$, $d/l = 1$, $b/l = 0$ and the Froude number is 0.25. In figure 11 the corresponding curves for incoming following waves (k_2 waves) are displayed and in figure 12 the curves for incoming

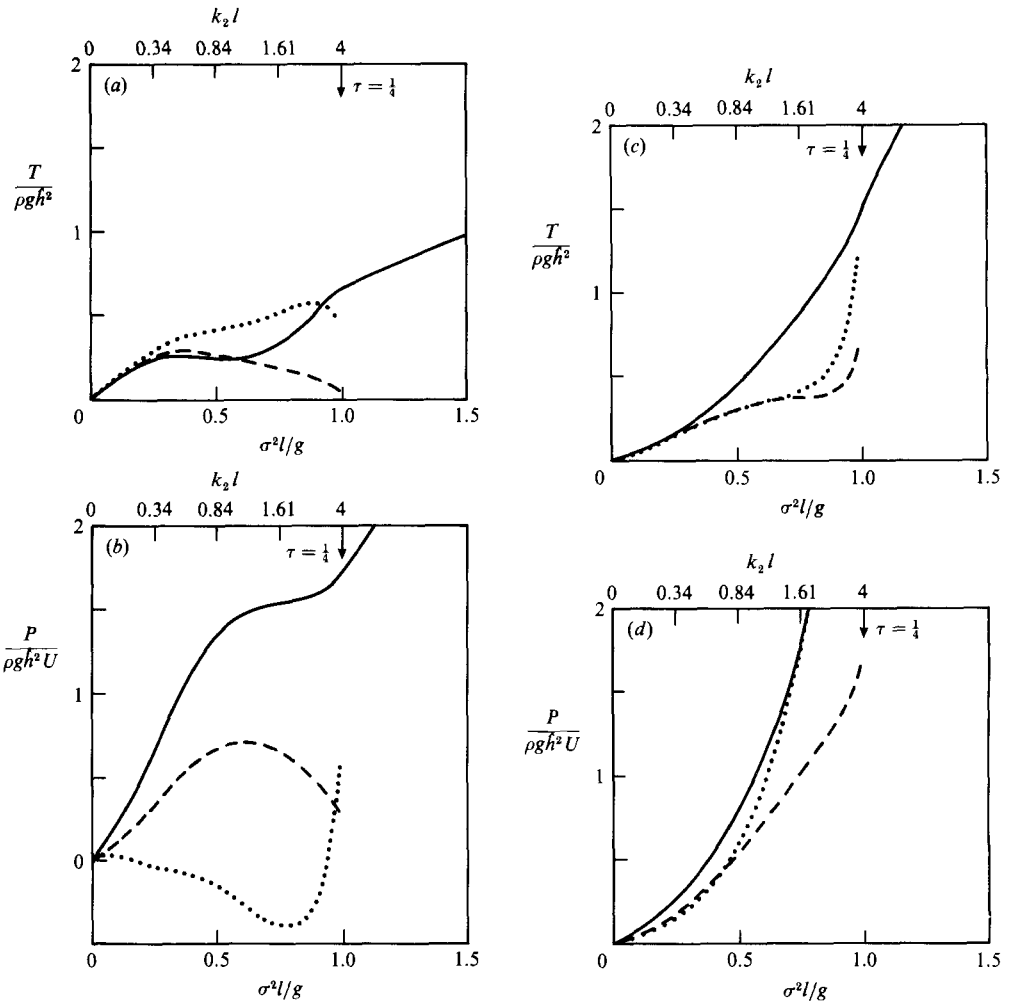

FIGURE 11. Same as figure 10, but foil oscillating in incoming following k_2 waves. ---, $\psi = -\frac{1}{2}\pi$, $\hat{a}_0/h = 1$. ···, $\psi = \pi$, $\hat{a}_0/h = 1$.

head waves for $Fr = 1$ and $\theta = 0.6$. We see that the three cases considered, oscillation in calm water and oscillation with two different incoming waves, give approximately the same curves for $T/\rho g\hat{h}^2$ when $k_0 l$ is less than about 0.5. Furthermore, we see from figures 10(*b*) and 11(*b*) that in pure heave the necessary power is considerably lowered in incoming waves. For incoming waves 90° out of phase with the foil oscillation the necessary power is close to zero and even negative.

In the general case, with incoming waves of all wave numbers, the display of the results becomes very complicated due to the large number of parameters in the problem. It also turns out that the solution is very sensitive to variation in several of the parameters. We shall therefore restrict ourselves to considering a foil moving in an incoming wave field without oscillating. The power P is then zero. In figure 13 are displayed values of the thrust due to incoming head waves and following waves for different values of the Froude number. We see that for following waves the picture is rather complicated, essentially due to the influence of $\tau = \frac{1}{4}$. For head waves the

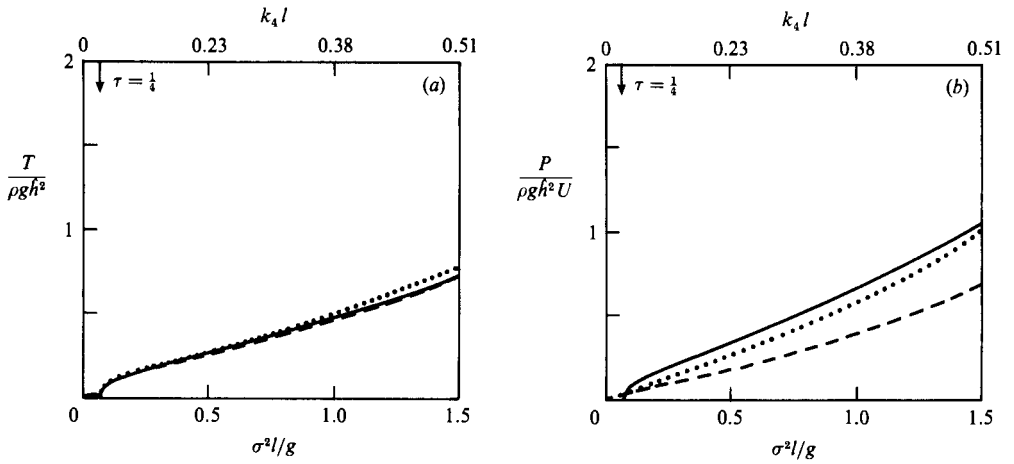

FIGURE 12. Same as figures 10(*c*), (*d*), but $Fr = 1$.

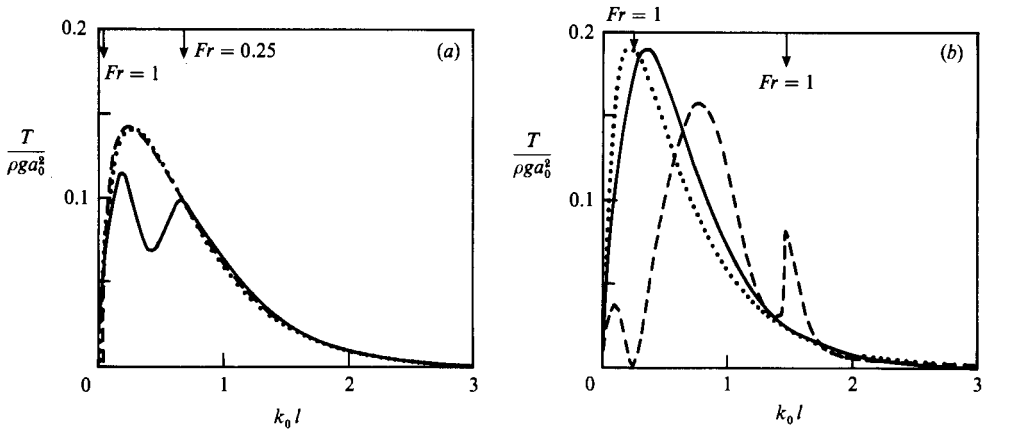

FIGURE 13. Thrust $T/\rho g a_0^2$ *vs.* wavenumber of incoming waves. No vertical motion of the foil. $d/l = 1$. ——, $Fr = 0.25$; – – –, $Fr = 1$; ···, $Fr = 5$. (*a*) Head waves, (*b*) following waves. The small arrows denote the occurrence of $\tau = \frac{1}{4}$.

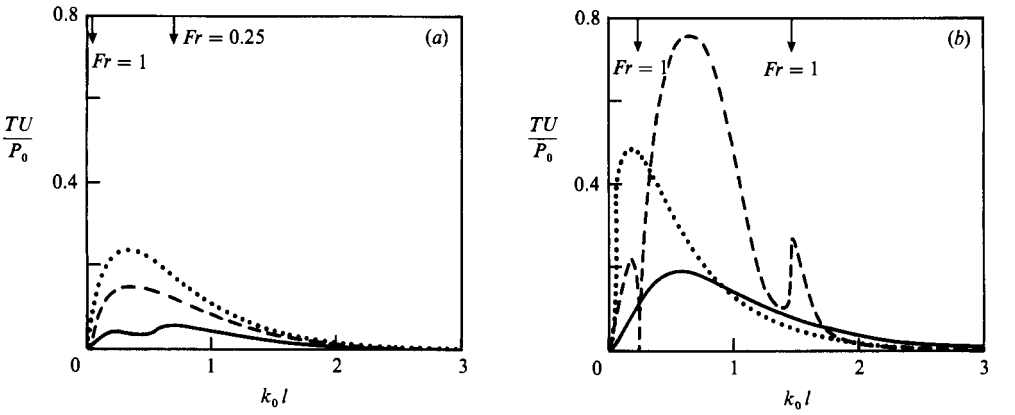

FIGURE 14. TU/P_0 *vs.* wavenumber of incoming waves. No vertical motion of the foil. $d/l = 1$. ——, $Fr = 0.25$; – – –, $Fr = 1$; ···, $Fr = 5$. (*a*) Head waves, (*b*) following waves. The small arrows denote the occurrence of $\tau = \frac{1}{4}$.

thrust is independent of the Froude number for $k_0 l > 0.7$. Figure 14 shows the value of TU/P_0 which, since $P = 0$, is the part of the wave energy power utilized for propulsion. The figures show that the largest amount of wave energy, up to 75%, may be utilized by a foil moving in following waves.

6.2. *Application on the propulsion of a ship by a foil propeller*

As a practical example of the theory we shall consider the propulsion of a ship by a foil propeller. We assume that the foil has a large aspect ratio so that by using the strip-theory approximation we may apply our two-dimensional theory. The ship is advancing with a speed U in regular waves. Due to the waves the ship, and thereby the foil, will undergo heaving and pitching motions with a frequency σ equal to the frequency of encounter. The oscillatory motion of the foil as well as the motion of the wave field relative to the foil will produce a forward thrust on the foil and thereby a forward thrust on the ship. We shall compute this thrust and the speed of the ship, U.

It is assumed that the heave motion of the ship is of the same order of magnitude as the amplitude of the incoming waves. This is true for both incoming head waves and incoming following waves, provided that the wavelength of the incoming wave, λ_0, is equal to or larger than the ship length L (Newman 1978; Wachnick & Zarnik 1965). Furthermore we assume a foil arrangement such that the foil moves downwards when the wave field velocity is upwards, i.e. $\psi = \frac{1}{2}\pi$ for incoming head waves and $\psi = -\frac{1}{2}\pi$ for incoming following waves.

We denote the thrust acting upon the foil by

$$T' = TB, \tag{6.13}$$

where T is the sectionwise thrust and B is the span of the foil. The latter will be assumed equal to the ship beam. For constant forward speed, T' must balance the total wave and viscous drag on the ship. The wave drag has two components which can be treated separately, viz. the drag due to the steady wave pattern generated by the ship, the wave resistance, and the added resistance due to scattering of incoming waves. The viscous drag is mainly frictional drag. The sum D of the drag due to the wave resistance and the frictional drag may be written in the form

$$D = \tfrac{1}{2}\rho C_{\mathrm{D}} S U^2, \tag{6.14}$$

where C_{D} is the drag coefficient and S is the wetted area of the vessel. A reasonable value of the drag coefficient for values of $U/(gL)^{\frac{1}{2}}$ less than about 0.3, is $C_{\mathrm{D}} = 2.5 \times 10^{-3}$ (see e.g. Newman 1977, p. 30). We approximate the wetted area of the vessel by the area of a half immersed circular cylinder with diameter B and length L, i.e. $S \approx \frac{1}{2}\pi BL$.

The added resistance D_{w} for a ship moving in head waves is discussed by Faltinsen *et al.* (1980) and may be written

$$D_{\mathrm{w}} = C_{\mathrm{w}} \rho g a_0^2 B^2 / L, \tag{6.15}$$

where C_{w} is a dimensionless function of $U/(gL)^{\frac{1}{2}}$ and λ_0/L. The maximal value of C_{w} (≈ 6) occurs for $\lambda_0/L \approx 1$. For longer or shorter waves C_{w} rapidly becomes smaller than 2. For a ship moving in following waves little is published about the relevant values of C_{w}. It is known that for very small values of U, C_{w} is negative. It seems reasonable that C_{w} is small for small and moderate values of $U/(gL)^{\frac{1}{2}}$.

	$\sigma^2 l/g$	$T/\rho g a_0^2$	C_w	U
Head waves	0.17	0.75	2	$16a_0 g/L$
Following waves	0.047	0.12	0	$8a_0 g/L$

TABLE 1. Values of $T/\rho g a_0^2$, C_w and U for $B/L = \frac{1}{8}$, $k_0 l = 0.1$, $d/l = 1$, $U/(gl)^{\frac{1}{2}} = 1$, $\hat{\theta} = 0$, $h/a_0 = 1$

Balance between T' and $D + D_w$ gives

$$T' = \frac{2.5\pi}{4} 10^{-3} \rho L B U^2 + C_w \rho g a_0^2 \frac{B^2}{L}, \tag{6.16}$$

or approximately

$$U = 23 \left(\frac{T}{\rho g a_0^2} - C_w \frac{B}{L} \right)^{\frac{1}{2}} a_0 \left(\frac{g}{L} \right)^{\frac{1}{2}}. \tag{6.17}$$

Let us furthermore assume that $B/L = \frac{1}{8}$, $d/l = 1$, $\hat{\theta} = 0$, $h/a_0 = 1$, $U(gl)^{\frac{1}{2}} = 1$ and $k_0 l = 0.1$. We set $C_w = 2$ in head waves and $C_w = 0$ in following waves. Values of $T/\rho g a_0^2$ are obtained from the computations in §5 (since $k_0 l \ll 1$). Table 1 demonstrates that the ship will move twice as fast in head waves as in following waves. If the ship length $L = 40$ m and the amplitude of the incoming head waves $a_0 = 0.5$ m, we find that $U \approx 4$ ms$^{-1} \approx 8$ knots. With $U \approx 4$ ms^{-1} and $U/(gl)^{\frac{1}{2}} = 1$, the half chord length is $l = 1.6$ m. Hence, $L/l = 25$, and $k_0 = 0.1$ corresponds to $\lambda_0/L = 2.5$.

7. Comparison with experiments and discussion

The only experiments we know about relevant to the present theory, were performed by Isshiki *et al.* (1984) (also published in part as report, Isshiki & Murakami 1983). Five of their experimental series are performed in set-ups similar to our theory, the other experiments are performed under other conditions. It turns out, however, that the amplitudes of the incoming waves in most series are rather large, having a magnitude close to the distance between the foil and the free surface, which leads to strong nonlinear effects. Therefore only one of the experimental series is directly comparable with the theory. The experiments are carried out in a tank 25 m × 1 m × 0.71 m (length × breadth × depth) with a wavemaker at one end of the tank. The foil is suspended by a carriage which moves horizontally with small resistance. The springs are stiff, so that the foil oscillations due to the incoming waves are small. As preliminary experiments the carriage and foil are pulled with constant speed in calm water, and the resistance of the system is determined as a function of speed. Then waves are incident upon the foil, which now moves forward solely due to the thrust caused by the waves ('free-running test'). The mean horizontal velocity is measured, and the thrust balancing the resistance is obtained by applying the results from the preliminary experiments.

We have simulated the experiments using the given data for the experimental set-ups. One problem is that the theory is valid for infinite depth whereas in the experiments the ratio of incoming wavelength to fluid depth may be up to about five. In the comparison we have adjusted the observed wavelength of the incoming wave so that the intrinsic frequency ω is the same in theory and experiments. This adjustment leads only to minor corrections. The amplitudes of the incoming

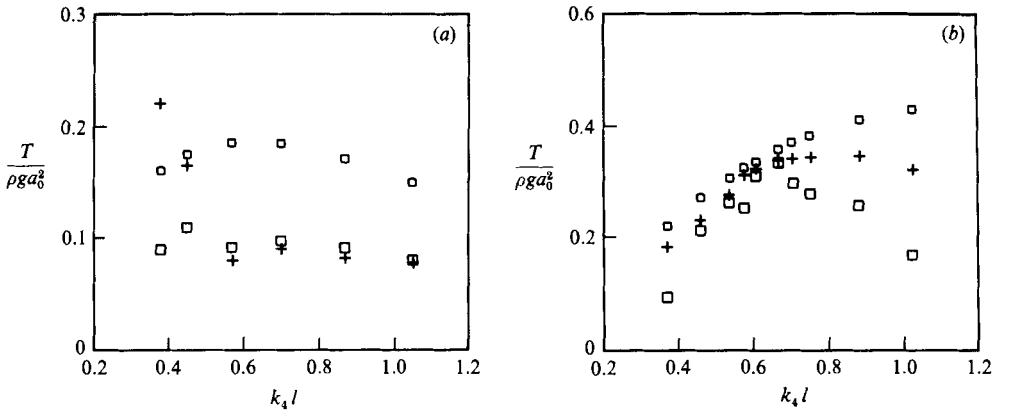

FIGURE 15. Thrust $T/\rho g h_0^2$ *vs.* wavenumber $k_4 l$ of incoming head waves. (*a*) $0.05 < Fr < 0.17$; (*b*) $0.15 < Fr < 0.38$. □, thrust obtained from experiments. Isshiki *et al.* (1984), figure 32; (*a*) $d/l = 0.8$, (*b*) $d/l = 0.3$. □, approximate theory, Wu (1972). +, present theory.

observed waves have a considerable scattering. In the comparison we have chosen the mean value of the amplitudes.

The thrust obtained for incoming head waves by the present theory and the experiments is presented in figure 15(*a*). The thrust obtained from simulations of the experiments by Wu's approximate theory (1972) are also shown. The submergence of the foil is $d/l = 0.8$ (in the experiments $l = 20$ cm and $d = 16$ cm). The amplitude of the incoming waves varies between 3.8 cm and 5 cm, i.e. $a/d \approx 0.3$. We find that the agreement between experiments and theory is good in most cases. For the lowest wavenumbers there are systematic discrepancies It is reasonable to suppose that the discrepancies are due to nonlinear effects which are not accounted for in the theory. To examine this more closely we have computed the values of $\frac{1}{2}|\gamma_0|/U$ for the cases displayed in figure 15. It is found that this quantity, which in the theory is assumed much smaller than unity, varies from about 1 to 13. It is especially large for $k_4 l < 0.5$, and explains the disagreements for these wavenumbers. A large value of $\frac{1}{2}|\gamma_0|/U$ means that the linearized modelling of the vortex wake is not valid, and that the Kutta condition at the trailing edge cannot be applied.

Figure 15(*b*) shows the results for one of the four series of experiments where the foil moves very close to the free surface. The incoming waves here are head waves and the submergence of the foil is $d = 6$ cm ($d/l = 0.3$). In this case $a/d \approx 0.8$ and we expect large nonlinear effects. Somewhat surprisingly, there are fairly good agreements between the theoretical and experimental results for moderate values of the wavenumber. Actually, in this and three other cases where the foil moves very close to the free surface, the theory and the experiments agree fairly well when, in addition to $\frac{1}{2}|\gamma_0|/U$ being of order unity, the computed influence of the foil on the wave field is relatively small. Since a_1 and a_3 are close to zero in all the experiments, the latter means that the amplitude of the reflected wave is small compared to a_0 and the amplitude of the transmitted wave is close to a_0.

For a small Froude numbers and the foil sited very close to the free surface, we find a kind of resonance. This is experienced by the thrust and the reflected wave amplitude varying rather rapidly close to certain values of the wavenumbers for the incoming waves. A detailed numerical study has revealed that resonance behaviour takes place for Froude numbers less than about 0.3 and d/l less than about 0.5. It

is also found that this resonance is most pronounced when $U \to 0$. The lowest minimum of the reflected wave amplitude then occurs for $k_0 l$ about 3 ($d/l = 0.3$). For increasing Froude number this minimum occurs for decreasing wavenumber. The experiments show no sign of this resonance, which is probably due to strong nonlinearity.

Isshiki (1982) has also prepared a simplified theory for taking into account the free surface. He applies the formulae in theory of Wu (1972), where the free surface is not taken into account, to calculate the lift and moment acting upon the foil. He then replaces the foil by two dipoles, sited at the centre of the foil, of strength equal to the calculated lift and moment, and calculates the amplitude of the waves generated by the dipoles. The momentum equation is then used to obtain the impact of the waves on the thrust. Isshiki has applied his theory for a deeply submerged foil, $d/l = 3$, which is moving without oscillation in incoming waves. His theory and our theory agree for very long incoming waves. However, for $k_0 l > 0.1$ the discrepancy between the two theories is more than 100%. For smaller values of d/l the disagreement is most likely larger still.

Appendix A: The $P(x)$ function

The $P(x)$ function in §3 may be considerably simplified for numerical evaluation. $P(x)$ is defined by (3.30) as

$$P(x) = -\int_{-\infty}^{-l} \exp(\mathrm{j}k\xi)\left[\frac{\mathrm{j}}{k\pi}\frac{\mathrm{d}}{\mathrm{d}\xi}\left[\frac{(\xi^2-l^2)^{\frac{1}{2}}}{x-\xi}\right]+\tilde{K}(x,\xi)\right]\mathrm{d}\xi, \tag{A 1}$$

where $\tilde{K}(x,\xi)$ is defined in §3 in form of a double integral. We consider the first part of (A 1), which we shall call $P_0(x)$. After some elementary algebra we find that $P_0(x)$ may be written

$$P_0(x) = -\frac{\mathrm{j}}{k\pi}\exp(\mathrm{j}kx)\,[xA_1(k)-(l^2-x^2)\,A_2(k)], \tag{A 2}$$

where

$$A_n(k) = \int_{-\infty}^{-l}\frac{\exp(\mathrm{j}k(\xi-x))}{(\xi-x)^n\,(\xi^2-l^2)^{\frac{1}{2}}}\mathrm{d}\xi \quad (n = 1, 2). \tag{A 3}$$

Applying the fact that the Hankel function of the second kind and of order zero for positive argument has the integral representation (Watson 1922, p. 180),

$$H_0^{(2)}(x) = \frac{2\mathrm{j}}{\pi}\int_1^{\infty}\frac{\exp(-\mathrm{j}xt)}{(t^2-1)^{\frac{1}{2}}}\mathrm{d}t, \tag{A 4}$$

we obtain,

$$A_1(k) = A_1(0)+\tfrac{1}{2}\pi\int_0^k \exp(-\mathrm{j}ux)\,H_0^{(2)}(ul)\,\mathrm{d}u, \tag{A 5}$$

$$A_2(k) = A_2(0)+\mathrm{j}kA_1(0)+\tfrac{1}{2}\mathrm{j}\pi\int_0^k (k-u)\exp(-\mathrm{j}ux)\,H_0^{(2)}(ul)\,\mathrm{d}u. \tag{A 6}$$

From (A 3)

$$A_1(0) = \frac{2}{(l^2-x^2)^{\frac{1}{2}}}\left[\arctan\left(\frac{l+x}{l-x}\right)^{\frac{1}{2}}-\tfrac{1}{2}\pi\right], \tag{A 7}$$

$$A_2(0) = \frac{\partial}{\partial x}A_1(0). \tag{A 8}$$

Introducing (A 5–A 8) into (A 2), applying a partial integration and manipulating with Hankel functions we finally obtain

$$P_0(x) = \frac{2}{\pi}\exp(\mathrm{j}kx)(l^2-x^2)^{\frac{1}{2}}\left[\tfrac{1}{2}\pi - \arctan\left(\frac{l+x}{l-x}\right)^{\frac{1}{2}}\right] + \tfrac{1}{2}H_1^{(2)}(kl)$$
$$-\tfrac{1}{2}\mathrm{j}xH_0^{(2)}(kl) - \tfrac{1}{2}(l^2-x^2)\exp(\mathrm{j}kx)\int_0^k \exp(-\mathrm{j}ux)H_0^{(2)}(ul)\,\mathrm{d}u. \tag{A 9}$$

The last term in (A 1), P_1, may by changing the order of integration be written

$$P_1(x) = -\frac{1}{\pi^2}\int_{-l}^{l}\frac{(l^2-\eta^2)^{\frac{1}{2}}}{x-\eta}\mathrm{d}\eta\int_{-\infty}^{-l}\exp(\mathrm{j}k\xi)K(\eta,\xi)\,\mathrm{d}\xi. \tag{A 10}$$

From (3.24) and (3.3), $K(\eta,\xi)$ may be written

$$K(\eta,\xi) = -\frac{1}{2}\left[\frac{1}{\eta-\xi-2\mathrm{j}d}+\frac{1}{\eta-\xi+2\mathrm{j}d}\right]$$
$$+\frac{\mathrm{j}}{(1-4\tau)^{\frac{1}{2}}}[k_1F_1(\eta-\mathrm{j}d,\xi-\mathrm{j}d)-k_2F_2(\eta-\mathrm{j}d,\xi-\mathrm{j}d)]$$
$$-\frac{\mathrm{j}}{(1+4\tau)^{\frac{1}{2}}}[k_3\overline{F_3(\eta-\mathrm{j}d,\xi-\mathrm{j}d)}-k_4\overline{F_4(\eta-\mathrm{j}d,\xi-\mathrm{j}d)}], \tag{A 11}$$

where
$$F_n(\eta-\mathrm{j}d,\xi-\mathrm{j}d) = \exp(-\mathrm{j}k_n\eta-k_nd)\int_{C_n}^{\eta-\mathrm{j}d}\frac{\exp(\mathrm{j}k_nu)}{u-\xi-\mathrm{j}d}\mathrm{d}u. \tag{A 12}$$

C_n, k_n and τ are defined in §3 and a bar denotes complex conjugate. Changing the order of integration and applying partial integration, we obtain

$$\int_{-\infty}^{-l}\exp(\mathrm{j}k\xi)K(\eta,\xi)\,\mathrm{d}\xi = \exp(-\mathrm{j}kl)\left\{[\tfrac{1}{2}\exp(v)E_1(v)]+\tfrac{1}{2}[\overline{\exp(-v)E_1(-v)}]\right.$$
$$+\frac{1}{(1-4\tau)^{\frac{1}{2}}}\left[\frac{k_1}{k_1+k}F_1(\eta-\mathrm{j}d,-l-\mathrm{j}d)-\frac{k_2}{k_2+k}F_2(\eta-\mathrm{j}d,-l-\mathrm{j}d)\right]$$
$$\left.+\frac{1}{(1+4\tau)^{\frac{1}{2}}}\left[\frac{k_3}{k_3-k}\overline{F_3(\eta-\mathrm{j}d,-l-\mathrm{j}d)}-\frac{k_4}{k_4-k}\overline{F_4(\eta-\mathrm{j}d,-l-\mathrm{j}d)}\right]\right\}. \tag{A 13}$$

Here v is given by
$$v = \mathrm{j}k(\eta+l-2\,\mathrm{j}d), \tag{A 14}$$

and the exponential integral $E_1(v)$ is defined in Abramowitz & Stegun (1972, p. 228).

Appendix B. The wave amplitudes in the far field

The wave amplitudes in the far field are derived from the complex velocity field (3.10)

$$u-\mathrm{i}v = \frac{\mathrm{d}f_0}{\mathrm{d}z}+\int_{-\infty}^{l}\gamma(\xi)\frac{\partial G}{\partial z}(z,\xi-\mathrm{i}d)\,\mathrm{d}\xi, \tag{B 1}$$

for $x\to\pm\infty$. Here $f_0(z)$ is the complex potential for the incoming wave and $G(z,z_0)$ is the vortex potential defined in §3. On the interval $(-l,\,l)$ $\partial G/\partial z$ reduces to terms of the form (3.4) which for $x\to\pm\infty$ become

$$\underset{z\to\pm\infty}{F_n(z,z_0)} = \exp(-\mathrm{i}k_nz)\int_{C_n}^{z}\frac{\exp(\mathrm{i}k_nu)}{u-\bar{z}_0}\mathrm{d}u \quad (z\to\pm\infty,\ n=1,2,3,4). \tag{B 2}$$

Here C_n and k_n are defined in §3. (B 2) is easily evaluated by contour integration.

The contribution from the wake is

$$\lim_{x \to \pm \infty} \gamma_0 \int_{-\infty}^{-l} \exp(\mathrm{j}k\xi) \frac{\partial G}{\partial z}(z, \xi - \mathrm{i}d)\, \mathrm{d}\xi. \tag{B 3}$$

The terms of the form (B 2) are evaluated by changing the order of integration, applying partial integration and contour integration. The remaining part of (B 3), due to terms of the form $1/(z-z_0)$ and $1/(z-\bar{z}_0)$, are found by contour integration. These terms tend towards zero for $x \to \infty$. For $x \to -\infty$ they are non-zero. They give, however, no contribution to the vertical displacement of the free surface. The final form of (B 1) is obtained by using (3.20). From this form the expressions for the amplitudes as given by (5.3) and (5.4) follow immediately.

We wish to acknowledge the financial support provided by the Norwegian Council for Science and the Humanities.

REFERENCES

ABRAMOWITZ, M. & STEGUN, I. A. 1972 *Handbook of Mathematical Functions.* Dover.

FALTINSEN, O. M., LIAPIS, N., MINSAAS, K. J. & SKJØRDAL, S. O. 1980 Prediction of resistance and propulsion of a ship in a seaway. *13th Symp. on Naval Hydrodyn.* The Shipbuilding Association of Japan.

GRUE, J. & PALM, E. 1985 Wave radiation and diffraction from a submerged body in a uniform current. *J. Fluid Mech.* **151**, 257.

HASKIND, M. D. 1954 On wave motion of a heavy fluid. *Prikl. Math. Mech.* **18**, 15.

ISSHIKI, H. 1982 A theory of wave devouring propulsion (1st report). Thrust generation by a linear Wells Turbine. *J. Soc. Nav. Arch. Japan* **151**, 54.

ISSHIKI, H. & MURAKAMI, M. 1983 A theory of wave devouring propulsion (3rd report). An experimental verification of thrust generation by a passive-type hydrofoil propulsor. *J. Soc. Nav. Arch. Japan* **154**, 125.

ISSHIKI, H., MURAKAMI, M. & TERAO, Y. 1984 Utilization of wave energy into propulsion of ships – wave devouring propulsion. *15th Symp. on Naval Hydrodyn.* National Academy Press, Washington, D.C.

JAKOBSEN, E. 1981 The foil propeller, wave power for propulsion. *2nd Intl Symp. on Wave and Tidal Energy.* BHRA Fluid Engineering, 363.

KÁRMÁN, TH. VON & BURGERS, J. M. 1934 *Aerodynamic Theory. A General Review of Progress.* ed. W. F. Durand. California Institute of Technology 1943.

LIGHTHILL, J. 1970 Aquatic animal propulsion of high hydrodynamical efficiency. *J. Fluid Mech.* **44**, 265.

MO, A. & PALM, E. 1987 On radiated and scattered waves from a submerged elliptic cylinder in a uniform current. *J. Ship Res.* **31**, 23.

NEWMAN, J. N. 1977 *Marine Hydrodynamics.* MIT Press.

NEWMAN, J. N. 1978 The theory of ship motions. *Adv. Appl. Mech.* **18**, 221.

WACHNIK, Z. C. & ZARNIK, E. E. 1965 Ship motion prediction in realistic short-crested seas. *Soc. Nav. Arch.* and *Marine Engnrs Trans.* **73**, 100.

WATSON, G. N. 1922 *A Treatise on the Theory of Bessel Functions.* Cambridge University Press.

WU, T. Y. 1961 Swimming of a waving plate. *J. Fluid Mech.* **10**, 321.

WU, T. Y. 1971*a* Hydromechanics of swimming propulsion. Part 1. Swimming of a two-dimensional flexible plate at variable forward speeds in an inviscid fluid. *J. Fluid Mech.* **46**, 337.

WU, T. Y. 1971*b* Hydromechanics of swimming propulsion. Part 2. Some optimum shape problems. *J. Fluid Mech.* **46**, 521.

WU, T. Y. 1972 Extraction of flow energy by a wing oscillating in waves. *J. Ship Res.* **16**, 66.